

THE ROLE OF TEP IN ESTUARINE HYDROSEDIMENTARY FUNCTIONING: IMPACT ON SETTLING VELOCITY OF AGGREGATES

Jean-Pierre Lefebvre^{1,2}, Xavier Mari¹, Thi Phuong Thao Do³ and Thuoc Văn Chu⁴

Transparent exopolymer particles (TEP) are widely recognized to promote sediment aggregation in eutrophic environments. Flocculation in presence of TEP of various suspended sediment concentrations of material sampled on the bank of the Cam River was quantified at the laboratory for turbulence level consistent with slack water and mid ebb conditions measured in the Cam River estuary during dry season of 2009. Stickiness and concentrations of TEP were let to naturally fluctuate by incubation (aging in the dark) for up to nine days. We found that the impact of turbulence on overall buoyancy of TEP-governed aggregation was always opposite between slack water and mid ebb conditions for any duration of incubation; always negative for slack water conditions but for 126 hours of incubation and significantly negative for mid ebb conditions but for 126 hours of incubation. Suspended sediment concentration (SSC) consistently limited aggregates buoyancy, negative or positive. We propose a conceptual model that relates measured and inferred parameters to observed hydrosedimentary processes.

Keywords: TEP, flocculation, estuary, oscillating-grid turbulence, LISST

INTRODUCTION

In order to evaluate the flux of cohesive sediments in natural environment, the concentration and the settling velocity of flocs must be known simultaneously. The settling velocity of a floc depends of its size and density, and of the turbulence within the flow. The assumption of a fractal dependence between density and size of floc is usually made (Kranenburg 1994). Two parameters govern flocculation of cohesive sediment in suspension in salt water: suspended sediment concentration (SSC) and turbulent shear stress (Dyer and Manning 1999, Manning and Dyer 1999, Winterwerp 1998, Winterwerp 2002). Further studies demonstrated that the settling velocity of aggregates in estuaries cannot be related to the size of the flocs only but must take into account the impact of organic matter on aggregation (van der Lee 2000).

Transparent Exopolymer Particles (TEP) are polysaccharidic exopolymers produced by phytoplankton and bacterioplankton. Their density ranges from 0.7 to 0.84 (Azetsu-Scott and Passow 2004). Because of their stickiness, TEP can aggregate mineral flocs and form mixed biological and mineral structures. The resulting aggregates are larger and less dense than the embedded mineral flocs (Logan et al. 1995, Passow et al. 2001). In estuaries, concentration and stickiness of TEP vary in time and space; stickiness increases with residence time while concentration decrease (Rochelle-Newall et al. 2010, Barrera-Alba et al. 2012; Mari et al. 2012). Despite recognized as crucial, the knowledge on influence of TEP on aggregation remains scarce which hindered efforts to model impact of organic matter in flocculation processes and at a larger scale hydrosedimentary functioning of eutrophic environments like estuaries (Voulgaris and Meyers 2004, Verney et al. 2009, Markussen and Andersen 2013).

The Red River delta (Vietnam) is under the influence of a tropical monsoon climate with wind direction dominantly from the south in April–September (wet season), and from the northeast in October–March (dry season). The Cam River is a tributary of the Van Uc River; the most Eastern main tributary of the Red River. The hydrosedimentary functioning of the Cam River Estuary was investigated during wet season of 2008 and dry season of 2009 (Lefebvre et al. 2012). High concentration of TEP were found during both dry and wet season (Mari et al. 2012). In order to assess the role played by TEP on flocculation processes, a study was conducted at the laboratory with controlled turbulence matching the levels measured at the mouth of the Cam River during the dry season of 2008 for slack water and mid ebb. Both used water and sediments were sampled during the dry season of 2013 in the vicinity of field measurement station; water in the plume and sediments, on the bank of the Cam River. The size distributions of aggregate were simultaneously measured by two LISST (Sequoia Scientific, Inc.). Furthermore, we extracted contributions of four levels of aggregation

¹ Institut de Recherche pour le Développement, France

² Hanoi University of Sciences, Hanoi, Vietnam

³ Institute of Environmental Technology, Hanoi, Vietnam

⁴ Institute of Marine Environment and Resources, Haiphong, Vietnam

(referred to as modes); flocculus, fine and coarse microflocs, and macroflocs from total class size distribution with the method described by Lefebvre et al. (2012). We deducted corresponding SSC for each mode and finally we assessed the equivalent buoyancy of each modes and the mass of sediment either settling or located at the free surface (suppressed mass sediment), for various incubation duration and turbulence corresponding to slack water and mid ebb conditions and average SSC ranging from 5 to 50 mg L⁻¹.

MATERIALS AND METHODS

Measurement protocol

Suspensions of 5, 10, 20, 30, 40 and 50 mg L⁻¹ were prepared in water incubated for 0, 1, 2, 5 and 10 days for stack water conditions and 0, 1, 5, 6 and 9 days mid ebb conditions. The suspension was homogenized manually by gentle stir of 10 s just before switching on the grid oscillation. The flocs size distribution (FSD) were measured once the equilibrium condition was reached. We considered the equilibrium condition met after 30 min, when the temporal variation of SSC measured by the two LISST were negligible

Water sampling

For each of the two tests, 20 liters of water were sampled in the plume of Cam River estuary and kept in polycarbonate bottles and brought back to the laboratory within 2 hours. Measured salinity was 20 for the two tests. In order to obtain various concentrations and stickiness properties for TEP, the samples were maintained at 24°C and kept in the dark in order to avoid photosynthesis and allow bacterial degradation of TEP, during 10 days per set of experiment (Rochelle-Newall et al. 2010, Mari et al. 2012). Before each test, only sub-microscopic TEP were kept by filtering the required volume of water through 47 mm diameter GF/C Whatman filters (nominal pore size = 1.2 µm) at low and constant vacuum pressure (< 200 mbar).

Sediment sampling

All the sediments needed for the study were sampled at one time in Haiphong city on the banks of the Cam River. The sediment was rinsed carefully with MilliQ water and dried at 60°C in a heat oven for a week. The sediment was then grounded and sieved through a 38 µm metal mesh. Only the fraction of sediment, which apparent diameter was less than 38 µm was kept for experimentation.

Oscillating-grid turbulence (OGT)

A cylindrical container (12.9 cm diameter and 15.3 cm height) was used. The oscillating grid diameter was 0.8 cm smaller than the container diameter and the stroke was 12 cm; the center of oscillation coinciding with the middle of water height. The grid mesh was 1.42 cm with a diameter of the bar of 0.38 cm. Two oscillation periods were selected: 12 and 3 s.

The Kolmogorov microscale corresponds to the smallest size, turbulent eddies can reach before viscous dissipation by the fluid. They are considered as of the same order of magnitude than the size of the largest flocs (Bouyer et al. 2004, Mietta et al. 2009, Lefebvre et al. 2012). Average Kolmogorov microscale (η) corresponding to turbulent kinetic energy (TKE) generated by grid oscillations of 3 and 12 s period were 272 and 1021 µm, respectively (Matsunaga et al. 1999, Jansen et al. 2003), which was close to those measured in Cam estuary during dry season of 2009 for mid ebb and slack water; 256 and 950 µm, respectively.

Measurements of flocs size distribution (FSD)

The water was continuously sampled 10 mm under the surface and 10 mm above the bottom of the container with a very low debit flow peristaltic pump and fitted online with two LISST (Laser In-Situ Scattering and Transmissometry, Sequoia Scientific, Inc.) (Agrawal and Pottsmith 1994). The first and last cells of the 32 logarithmic spaced scale of equivalent spherical diameter (ESD) were discarded (Traykovski et al. 1999). LISST type B and C were used for the near bottom and near surface analysis, respectively. The corresponding limited ESD ranged from 1.18 to 169 µm for type B and 2.25 to 322 µm, for type C. The analysis period was 10 s and measurements were smoothed by 30 s moving average.

Suspended Sediment Concentration

The SSC is related to the attenuation of laser beam (c) emitted by the LISST at the wavelength of 670 nm (Guillén et al. 2000, Ganju et al. 2007, Fettweis 2008, Hill et al. 2011, Neukermans et al. 2012). Following Agrawal et al. (2008):

$$c = a 1.13\alpha \frac{SSC}{d_{32}} + b \quad (1)$$

where d_{32} is the Sauter mean diameter and α a particle shape parameter and a and b , the calibration parameters for each LISST.

Beam attenuations of each LISST was measured for SSC of sieved sediment ranging from 25 to 200 mg L⁻¹. The minimum measurable SSC was 2.8 mg L⁻¹. The Sauter mean diameter for the sieved particles was found equal to 1.3 μ m and the associated shape factor α was found equal to 0.316.

Decomposition of FSD into modes

In natural environments, suspension even of monomodal distribution of particles, usually produces multi-modal size distribution. Each mode can be identified according to its level of arrangement. Flocculus are constituted by some individual particles strongly bound together by cohesive properties of the mineral. Microflocs are aggregation of flocculus. Because larger microflocs may be also constituted by smaller microflocs, we distinguish fine microflocs and coarse microflocs. Finally, macroflocs are larger arrangement comprising a significant amount of organic matter. Because these modes overlap; for example, fine microflocs constituted by numerous flocculus may be larger than small coarse microflocs constituted of few small fine microflocs, we chose to determine the optimum decomposition of size distribution of volume concentration into four modes: flocculus, fine microflocs, coarse microflocs and macroflocs by use of a method proposed by Lefebvre et al. (2012) that allows variation for parameters of each mode within fuzzy boundaries and allowing overlapping. The size distribution of volume concentration of suspended solid material (C_{vol}) was obtained by normalizing the class size distribution of volume concentration with the width of each class size (Jouon et al. 2008):

$$C_{vol}(D_i) = \frac{C_V(\sigma_{\min i} \leq \sigma_i < \sigma_{\max i})}{\sigma_{\max i} - \sigma_{\min i}} \quad (2)$$

with D_i , the median diameter of the i^{th} class size. The volume concentration distribution is interpolated over N logarithmically spaced ESD ($N = 291$) and scaled:

$$S_{N,i} = \frac{C_{vol,i}}{\sum C_{vol,i}} \quad (3)$$

S_N is consistent with a statistical distribution can modeled as a sum of I randomly-spaced Gaussian functions:

$$S_N = \sum_{i=1}^I \frac{\alpha_i}{\sqrt{2\pi\sigma_i^2}} \exp -\frac{(d_i - \delta_i)^2}{2\sigma_i^2} \quad (4)$$

The optimal number of elementary functions ($I \leq 100$) and the corresponding parameters ($\alpha_i, \delta_i, \sigma_i^2$) are obtained by recursive expectation-maximization (EM) algorithm (Dempster et al. 1977). Based on fuzzy-logic criteria, the I Gaussian functions are merged into four modes: flocculus, fine microflocs, coarse microflocs and macroflocs. Maximum sizes about 7 μ m, 15 μ m and 100 μ m, for the three first modes and macroflocs are larger than 100 μ m but their maximum size spanned over the LISST maximum detection size.

SSC of modes

Due to the transparency of TEP, LISST only measures mineral fraction of aggregates. Neither the actual size of the aggregate nor its density can be strictly determined without assumption of the quantity of TEP inside (within the porosity) and outside the mineral floc. Assuming a fractal dependence between size and density for aggregates, the density of an aggregate of size D constituted of seeds of size D_s (taken equal to the Sauter d_{32}) and density ρ_s (2600 kg m⁻³) is calculated (Kranenburg 1994) as:

$$\rho = \rho_w + (\rho_s - \rho_w) \left(\frac{D}{D_s}\right)^{nf-3} \quad (5)$$

The fractal dimension nf varies from 3 (no porosity) for the smallest particles to 2. Following Khelifa and Hill (2006), nf is expressed as a function of aggregate size ranging from 3 for primary particles size D_s to nf_{\min} for aggregates larger or equal to D_{fc} :

$$nf = 3 \left(\frac{D}{D_s}\right)^{\frac{\log(nf_{\min}/3)}{\log(D_{fc}/D_s)}} \quad (6)$$

Combining Eq. 5 with the expression for the dry mass of a floc of equivalent spherical diameter D :

$$M_{\text{dry}} = \frac{\pi}{6} D^3 \rho_s \frac{\rho - \rho_s}{\rho_w - \rho_s} \quad (7)$$

the SSC for a N_i flocs per unit volume for flocs of ESD D_i is obtained as:

$$\text{SSC} = \frac{\pi}{6} \rho_s \sum_i N_i D_i^3 \left(\frac{D_i}{D_s} \right)^{nf-3} \quad (8)$$

Assuming that the SSC associated to aggregates larger than the maximum detection size of the LISST could be neglected, SSC calculation based on beam attenuation (Eq. 1) must equate the one based on the fractal assumption (Eq. 8) extended to all the range of detection of the LISST. In order to solve Eq. 8, we substitute to D_i and N_i for the 30 retained class size of the LISST, the D_{50m} and N_m of the four modes m :

$$\text{SSC} = \zeta \frac{\pi}{6} \rho_s \sum_m D_{50m}^3 N_m \left(\frac{D_{50m}}{D_s} \right)^3 \left(\frac{D_{50m}}{D_s} \right)^{\beta-3} \quad (9)$$

with ζ , a calibration factor depending of the instrument and $\beta = \frac{\log(nf_{\min}/3)}{\log(D_{fc}/D_s)}$. Eq. 9 is solved iteratively for β with an additional assumption that the aggregation size distribution at a given location (near surface or near bottom) and incubation duration does not vary significantly for the range of average SSC.

Settling Velocity

The gradient or Fickian diffusion model assumes that the mixing flux is proportional to the concentration gradient. In the mixing tank, where horizontal gradients of SSC are negligible, the model simplifies as:

$$\frac{\partial \text{SSC}}{\partial t} = \frac{\partial}{\partial z} \left(K_z \frac{\partial \text{SSC}}{\partial z} + w_s \text{SSC} \right) \quad (10)$$

with K_z , the vertical turbulent diffusivity and w_s , the settling velocity of aggregates. If aggregates size and density do not vary during their displacement, w_s remains constant along the water column. When an equilibrium is reached, ($\frac{\partial \text{SSC}}{\partial t} = 0$), Eq. 10 can be solved for a height z :

$$\frac{\partial \text{SSC}}{\partial z} = - \frac{w_s}{K_z} \text{SSC} \quad (11)$$

Since K_z is decreasing upward in upper half of the container and downward in lower half for OGT, an equilibrium is met whether w_s is positive or negative. The vertical turbulent diffusivity express as:

$$K_z = \frac{v_t}{Sc_t} \quad (12)$$

with v_t , the turbulent (eddy) viscosity and Sc_t , the turbulent Schmidt number. The turbulent viscosity is obtained from standard k - ϵ model:

$$v_t = C_\mu \frac{k^2}{\epsilon} \quad (13)$$

with $C_\mu = 0.09$. Based on turbulent Schmidt number modeling (Kerssens et al. 1979, Tsujimoto 2010):

$$Sc_t^{-1} = 1 + 1.54 \left(\frac{w_s}{u_*} \right)^{2.12} \quad (14)$$

Approximating $u_* \sim \sqrt{\frac{3}{2}k}$, Eq. 14 simplifies as:

$$Sc_t^{-1} \sim 1 + \frac{w_s^2}{k} \quad (15)$$

with k , the turbulent kinetic energy (TKE). For OGT, following Matsunaga et al. (1999), dimensionless TKE (\hat{k}) and dimensionless TKE dissipation rate ($\hat{\epsilon}$) can be expressed in an analytical form as:

$$\hat{k} = \left(\frac{\hat{z}}{z_0} + 1 \right)^{-\frac{2}{r}} \quad (16.a)$$

$$\hat{\varepsilon} = \left(\frac{\hat{z}}{z_0} + 1\right)^{-\frac{3+r}{r}} \quad (16.b)$$

Corresponding dimensional parameters can be written for z pointing upward from the center of oscillation as:

$$k = k_0 \left(\frac{\varepsilon_0}{k_0^{3/2} z_0} |z| + 1\right)^{-\frac{2}{r}} \quad (17.a)$$

$$\varepsilon = \varepsilon_0 \left(\frac{\varepsilon_0}{k_0^{3/2} z_0} |z| + 1\right)^{-\frac{3+r}{r}} \quad (17.b)$$

with ε_0 , k_0 and z_0 being functions of oscillation frequency, mesh size of the grid and stroke, only. From Eq. 11, with SSC measured near surface and near bottom at two symmetrical heights (z_s and $-z_s$) from the mean oscillation height, SSC at a height z is obtained as:

$$\ln \text{SSC} = -\text{sign } z \text{ sign } w_s \frac{r z_0}{C_\mu} \text{atan} \frac{|w_s|}{k_0^{0.5}} \left(\frac{\varepsilon_0}{k_0^{1.5} z_0} z + 1\right)^{\frac{1}{r}} + C \quad (18)$$

with $C = \frac{1}{2}(\ln \text{SSC}_{-z_s} + \ln \text{SSC}_{z_s})$. The overall settling velocity is obtained by solving Eq. 18:

$$w_s = k_{z_s}^{0.5} \tan \frac{C_\mu}{2r z_0} (\ln \text{SSC}_{-z_s} - \ln \text{SSC}_{z_s}) \quad (19)$$

The average SSC between the two measurement heights ($\text{SSC}_{\text{integrated}}$) is obtained by numerical integration of Eq. 198. The calculated settling velocity depends not only of water and aggregates density, aggregates size but also to the impact of turbulence generated by the settling aggregates on the exerted drag force (Raudkivi 1976).

Suppressed sediment mass

The suppressed sediment mass corresponds to the mass of material either deposited on the bottom or floating at the free water surface. It depends both on the buoyancy and distribution of aggregates and on turbulence. We approximated the suppressed sediment mass as the mass of sediment located either below 10 mm above the bottom ($z < -z_s$) or above 10 mm under the surface ($z > z_s$). It was obtained from the difference between $\text{SSC}_{\text{average}}$ and $\text{SSC}_{\text{integrated}}$, measured at equilibrium:

$$M_{\text{suppressed}} = \frac{\pi}{4} \phi^2 (h \text{SSC}_{\text{average}} - 2z_s \text{SSC}_{\text{integrated}}) \quad (20)$$

with h, the height of water and ϕ , the container diameter.

RESULTS

No major impact on the controlled parameters was observed on median size for each mode (Table 1) with exception of median size of fine microflocs (Fig. 1). For both slack water and mid ebb conditions, median size of near surface aggregates was slightly lower than near bottom for every mode but macroflocs. This exception was likely due to the difference of measurement span of the two LISST used. A limited increase in coarse microflocs median size and decrease in macroflocs was observed between slack water conditions and mid ebb conditions. The size always increased after 24 hours of incubation. Flocculus median size tended to decrease with increasing $\text{SSC}_{\text{average}}$ (not shown).

Table 1. Median equivalent spherical diameter for each mode for slack water and mid ebb conditions near surface and near bottom, averaged for incubation duration and $\text{SSC}_{\text{average}}$. Standard deviations are indicated between brackets.				
Modes	Slack water		Mid ebb	
	near surface	near bottom	near surface	near bottom
flocculus	4.3 (0.5)	4.7 (0.9)	4.9 (0.3)	4.9 (0.5)
fine microflocs	8.3 (2.0)	8.4 (1.5)	9.9 (0.2)	9.5 (0.5)
coarse microflocs	27.3(2.5)	33.3 (8.7)	29.1 (1.0)	36.6 (4.1)
macroflocs	287.2(51)	127.1 (15)	209.0 (53)	123.3 (32)

The trend for fractal dimensions obtained from partition of SSC related to modes (Eqs. 6 and 9) are shown on Fig. 2. For a same ESD, aggregates measured near bottom were always less dense than

those measured near surface, where their fractal dimensions were close to those usually used in studies on marine flocculations. For comparison purpose, n_f used by Khelifa and Hill (2006) are reported on Fig. 2.

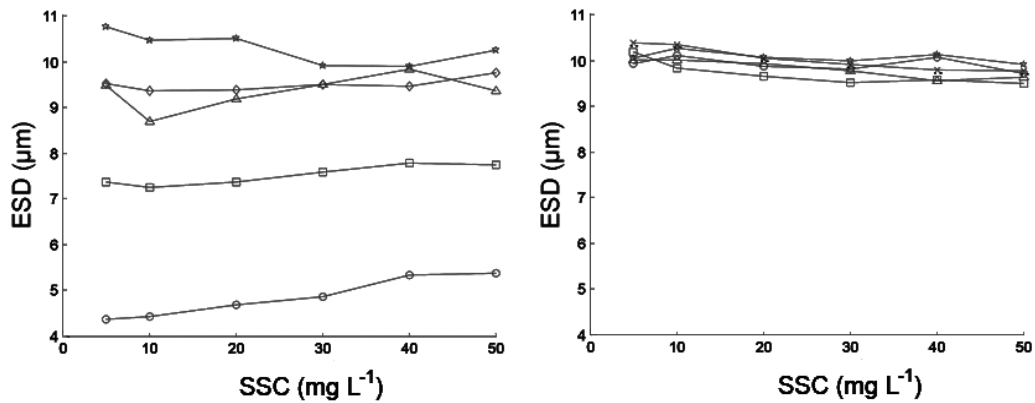


Figure 1. Median equivalent spherical diameter for near surface fine microflocs for slack water conditions (left) and mid ebb conditions (right) without incubation (O) and incubation of 24 hours (□), 48 hours (◇) 120 hours (△), 144 hours (×) and 216 hours (☆) for $SSC_{average}$ ranging for 5 to 50 $mg L^{-1}$.

Although moderately, the turbulence impacted flocs fractal dimensions; near surface, aggregates were denser for slack water conditions than for mid ebb conditions. This trend was reversed for near bottom aggregates. Because of the direction for K_z , in the upper half of the container, turbulent vertical diffusivity tended to transport light sediment above the height for near surface measurement, toward the surface and in the lower half of container, positive buoyancy aggregates were trapped by turbulence, pushing them downward.

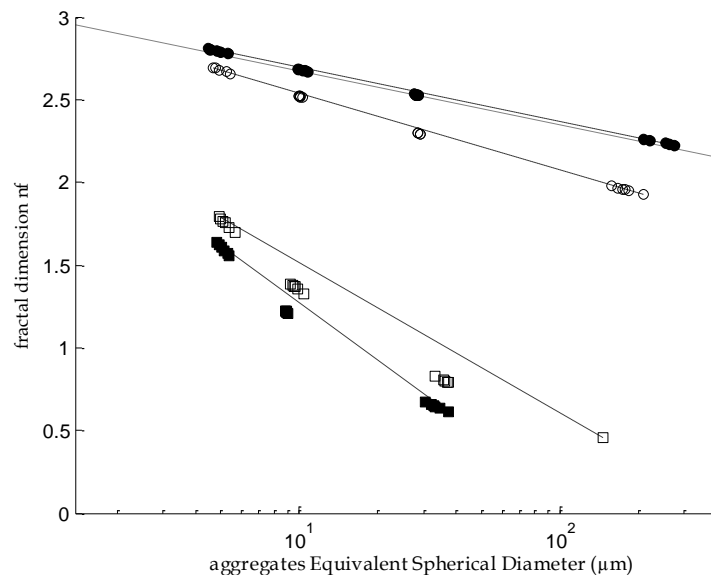


Figure 2. Fractal dimension for aggregates measured near surface (circle) and near bottom (square) for slack water conditions (empty markers) and mid ebb condition (filled markers).

The result showed on Fig. 2 indicates that two populations of aggregates coexisted: aggregates with fractal dimension close to the one estimated for mineral flocculation and low density aggregates impacted by TEP.

The equivalent settling velocity showed an opposite trend for every tested incubation duration, between TKE corresponding to mid ebb and to slack water. For mid ebb conditions, the flocs velocity were mostly upward with exception for incubation duration of 120 hours, and of order of magnitude of

0.1 mm s⁻¹. For slack water conditions, the settling velocity was of order of 0.01 mm s⁻¹, with upward sediment transport for incubation time longer or equal to 120 hours. The trend for magnitude of sediment transport was a decreased with increase in average SSC (Fig. 3).

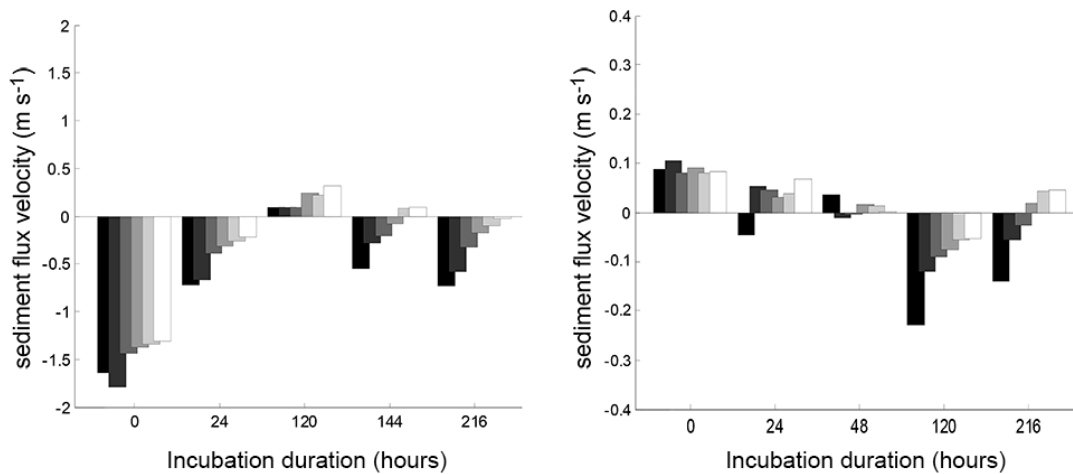


Figure 3. Sediment velocity for slack water conditions (left) and mid ebb conditions (right) for incubation durations up to 216 hours and SSC_{average} of 5, 10, 20, 30, 40 and 50 mg L⁻¹ (from black to white).

The change in direction was consistent with transfer of material from fine aggregates (flocculus and fine microflocs) to coarse microflocs, and macroflocs near surface for slack water conditions. Also, near bottom for mid ebb conditions, the proportion of coarse microflocs increased during the first 120 hours incubation and then decreased (Fig. 4).

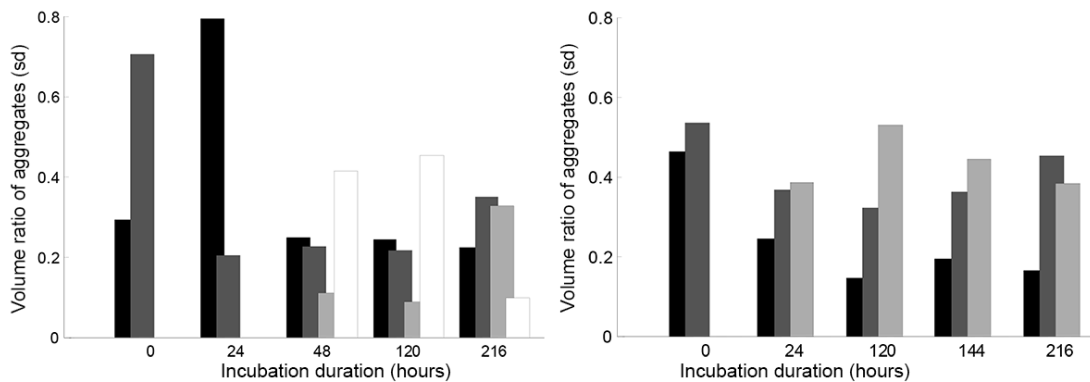


Figure 4. Proportion of flocculus (black), fine microflocs (dark gray), coarse microflocs (light gray) and macroflocs (white) in the measured aggregate volume near surface for slack water conditions (top) and near bed for mid ebb conditions (bottom) for SSC_{average} = 30 mg L⁻¹.

Due to the decrease in density of aggregates with increase of size, the transfer of sediment from fine aggregates to macroflocs had a more limited impact on SSC than the transfer from fine aggregates to coarse microflocs (Fig. 5).

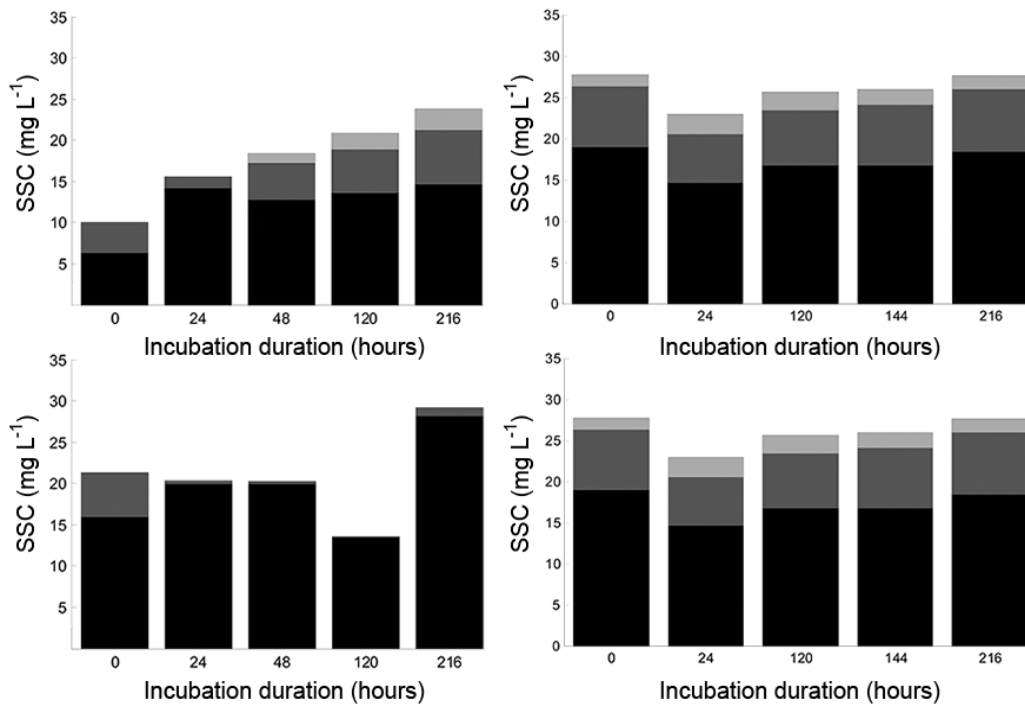


Figure 5. Suspended sediment concentration for flocculus (black), fine microflocs (dark gray) and coarse microflocs (light gray) for near surface (top) and near bottom measurements (bottom) for slack water (left) and mid ebb conditions (right), for $SSC_{average} = 30 \text{ mg L}^{-1}$.

The maximum suppressed sediment mass was calculated for each $SSC_{average}$ tested using Eq. 20. The incubation duration corresponding to the smallest suspended mass at equilibrium was retained for the calculation. It showed the same trend for slack and mid ebb conditions of an increase in maximum suppressed sediment mass for increasing average SSC up to $SSC_{average} = 30 \text{ mg L}^{-1}$ and was constant for higher $SSC_{average}$. The trend was similar for slack water conditions and mid ebb conditions but always of more limited amplitude for slack water conditions (Fig. 6).

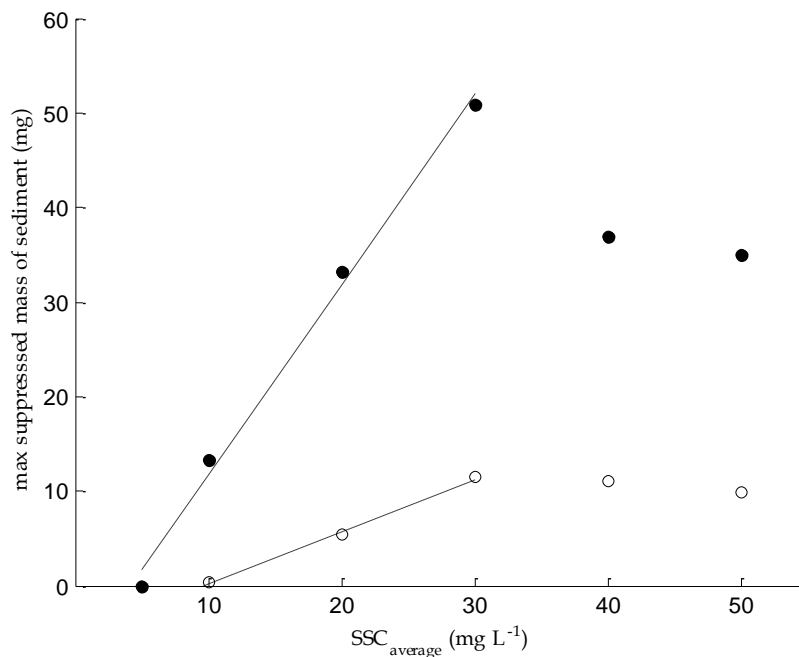


Figure 6. Maximum suppressed sediment mass for slack water conditions (○) and mid ebb conditions (●)

DISCUSSION

Due to the nature of optical measurements, properties of the aggregates solid fraction only were assessed. In particular, flocs bound together by transparent TEP matrix appeared as individual objects. TEP can also combine with flocs inside its porosity modifying its packing. Although no assumption was made in this study, it is likely that the quantity of TEP inside porosity and outside the flocs are related.

The impact of TEP on aggregation process varied with the three controlled parameters: average SSC, level of TKE and incubation duration. Global efficiency of TEP can be considered as a function of two characteristics; their abundance and stickiness. Stickiness increases with incubation after 48 hours while concentration decreases (Rochelle-Newall et al. 2010). In order to gain insight of observed behaviors, we take advantage of decomposition of distributions of number of aggregates per class size of the LISST.

The highest level of TKE was selected to match the depth averaged TKE dissipation rate estimated in situ for mid ebb (van der Lee et al. 2009, Lefebvre et al. 2012), although, it is questionable how close field measurements can be reproduced with OGT, characterized by marked variations of turbulence with depth in the container. Moreover, since TEP have positive buoyancy, the turbulent diffusivity in the upper half of the container accelerate their transport toward the surface. For the low turbulence levels used, it is unlikely that turbulent diffusivity directed downward in the lower half of the container can significantly prevent TEP from ascending.

Obtained results can be explain by a conceptual TEP aggregation efficiency (TAE) model (Fig. 7). Because it has been shown that measured sedimentation depended to every investigated parameters, the conceptual model must include TEP parameters; their stickiness and concentration, sediment concentration and turbulence. TEP parameters vary with incubation; stickiness increases while concentration decreases. For TEP aggregate sediment, the two objects must collide. The frequency of collision between TEP and sediments depends on their concentration, and this frequency can be enhanced by turbulence induced agitation. When sediments are aggregated with TEP, the organic bounds must withstand the turbulent shear stress and the shear stress due to unevenly located mass. For a given level of turbulence, a threshold value corresponding to the stickiness able to withstand the turbulent shear stress must exist. For lower value stickiness has no influence on aggregation and for higher value, the resulting stickiness hindered by turbulent shear stress allow aggregation. Not only the stickiness of TEP must hold the turbulent shear stress but also the equivalent mechanic resistance of an aggregate. former from unevenly located mass, it has also to resist to torque strength.

We observed a variation in ratio of mode with incubation duration which was consistent with the assumption that macroflocs can be formed by many TEP of low stickiness, and coarse microflocs, with less TEP of higher stickiness. This shift in mode repartition impacts strongly the sediment fluxes because the difference in density between coarse microflocs and macroflocs. When action of turbulence is no longer negligible, it can affect the two parameters of TAE. The TEP-sediment collision frequency must take into account the agitation generated by turbulence, which enhances collisions.

For stack water conditions, the influence of turbulence is negligible. The collision between TEP and sediment were mostly related to relative volume concentration of TEP and SSC and coarse microflocs and macroflocs were not broken up by turbulence although they still were broken up by torque strength, increasing statistically with increasing SSC. The increase in coarse microflocs and macroflocs from 0 to 120 hours of incubation and the following decrease was consistent with variation of TAE with its maximum for 120 hours of incubation. Because the TEP-sediment collision frequency was low, the mass of affected sediment was also low. The observed settling was due to the limited amount of created aggregates which increased up to the maximum of TAE, when sediment transfer upward were observed and then decreased in amplitude and became directed upward further. The limited variation of equivalent sediment velocity in still water is due to the limited dynamics for TAE resulting of balanced influence of decrease TEP concentration and increase of stickiness with incubation duration.

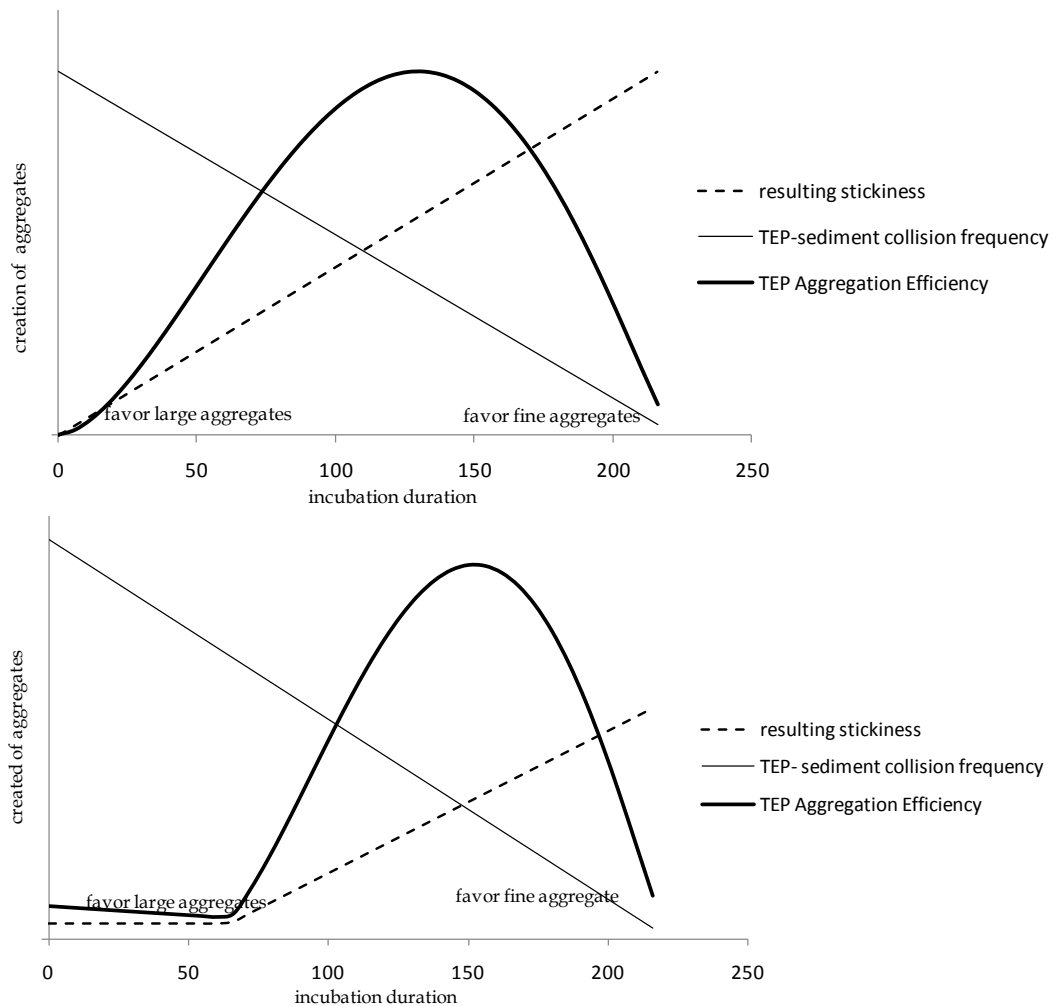


Figure 7. Conceptual model for TEP Aggregation Efficiency (TAE) without significant influence of TKE on TEP (top) and TKE with enhancing collision probability and limiting impact of stickiness on aggregation (bottom).

CONCLUSIONS

The decomposition of class size distribution of the LISST into modes (flocculus, fine microflocs, coarse microflocs and macroflocs) allowed to address impacts of TEP on aggregation. These decompositions were extended to suspended solid concentration. Taking advantage of controlled oscillating-grid turbulence, selecting two turbulence levels close to those measured at slack water and mid ebb of the estuary during the dry season of 2009, we observed significant changes in impact of TEP on aggregation for various quantities and stickiness properties of TEP obtained by incubation of sampled littoral water. We observed that the action of TEP on aggregation concerned not only large aggregates but also smaller ones; fine and coarse microflocs.

We found that the variation with incubation of the two main properties of TEP; their stickiness and concentration tended to compensate by one another. It resulted in maintaining most of the sediment into the water column during slack water. The turbulence corresponding to mid ebb conditions, by limiting action of stickiness of TEP and favoring the collision between TEP and sediment introduced an imbalance that resulted in an overall aggregation of positive buoyancy, for most of incubation duration. The agreement between measurement and assumptions leads us to propose a conceptual model for assessing the impact of TEP on aggregation in estuaries.

ACKNOWLEDGMENTS

We are grateful to the Institute of Marine Environment and Resources (IMER), to the University of Science and Technology of Hanoi (USTH) and to the French Research Institute for Development (IRD) for their technical and administrative support during the realization of this work.

REFERENCES

- Agrawal Y.C., Pottsmith H.C. 1994. Laser diffraction particle sizing in STRESS. *Continental Shelf Research*, 14(10/11), 1101–1121.
- Agrawal Y.C., Whitmire A., Mikkelsen O.A., Pottsmith H.C. 2008. Light scattering by random shaped particles and consequences on measuring suspended sediments by laser diffraction. *Journal of Geophysical Research*, 113, C04023.
- Azetsu-Scott K., Passow U. 2004. Ascending marine particles: Significance of transparent exopolymer particles (TEP) in the upper ocean. *Limnology and Oceanography*, 49(3), 741–748.
- Barrera-Alba J.J., Oliveira Moser G.A., Flores Ganesella S.M., Prado Saldanha-Corrêa F.M. 2012. Role of Transparent Exopolymer Particles on Phytoplankton Dynamics in a Subtropical Estuary, Cananéia-Iguape (SP, Brazil). *Open Journal of Marine Science*, 2, 25-32.
- Bouyer D., Liné A., Do-Quang Z. 2004. Experimental analysis of floc size distribution under different hydrodynamics in a mixing tank. *American Institute of Chemical Engineers Journal*, 50, 2064–2081.
- Dempster A.P., Laird N.M., Rubin D.B. 1977. Maximum Likelihood from Incomplete Data via the EM Algorithm. *Journal of the Royal Statistical Society: Series B (Methodological)*, 39(1), 1–38.
- Dyer K.R., Manning A.J. 1999. Observation of the size, settling velocity and effective density of flocs, and their fractal dimensions. *Journal of Sea Research*, 41, 87–95.
- Fettweis M. (2008). Uncertainty of excess density and settling velocity of mud flocs derived from in situ measurements. *Estuarine, Coastal Shelf Sci*, 78, 426–436.
- Guillén J., Palanques A., Puig P., Durrieu de Madron X., Nyffeler F. 2000. Field calibration of optical sensors for measuring suspended sediment concentration in the western Mediterranean. *Scientia Marina*, 64(4), 427–435.
- Ganju N.K., Schoellhamer D.H., Murrell M.C., Gartner J.W., Wright S.A. 2007. Constancy of the relation between floc size and density in San Francisco Bay. In Maa J.P.-Y., Sanford L.P., Schoellhamer D.H. (Eds.), *Estuarine and Coastal Fine Sediments Dynamics*. Elsevier Science B.V., Amsterdam, pp. 75–91.
- Hill P.S., Boss E., Newgard J.P., Law B.A., Milligan T.G. 2011. Observations of the sensitivity of beam attenuation to particle size in a coastal bottom boundary layer. *Journal of Geophysical Research*, 116, C02023, 14 pp.
- Jansen J.G., de Souza L.B.S., Schulz H.E. 2003. Kinetic energy in grid turbulence: Comparison between data and theory. *Journal of the Brazilian Society of Mechanical Sciences and Engineering*, 25(4), 347-351.
- Jouan A., Ouillon S., Douillet P., Lefebvre J.-P., Fernandez J.-M., Mari X., Froidefond J.-M. 2008. Spatio-temporal variability in suspended particulate matter concentration and the role of aggregation on size distribution in a coral reef lagoon. *Marine Geology*, 256(1–4), 36–48.
- Kerssens P.J.M., Prins A., van Rijn L.C. 1979. Model for suspended sediment transport. *Journal of the Hydraulics Division*, 105(5), 461–476.
- Khelifa A., Hill P.S. 2006. Models for effective density and settling velocity of flocs. *Journal of Hydraulic Research*, 44(3), 390–401.
- Kranenburg C. 1994. The fractal structure of cohesive sediment aggregates. *Estuarine and Coastal Shelf Sciences*, 39, 451–460.

- Lefebvre J.-P., Ouillon S., Vinh V.D., Arfi R., Panché J.-Y., Mari X., Thuoc C.V., Torrétion J.-P. 2012. Seasonal variability of cohesive sediment aggregation in the Bach Dang-Cam Estuary Haiphong (Vietnam). *Geo-Marine Letters*, 32, 103–121.
- Logan B.E., Passow U., Alldredge A.L., Grossart H.-P., Simon M. 1995. Rapid formation and sedimentation of large aggregates is predictable from coagulation rates (half-lives) of transparent exopolymer particles (TEP). *Deep-Sea Research*, 42(1), 203–214.
- Manning A.J., Dyer K.R. 1999. Laboratory examination of floc characteristics with regard to turbulent shearing. *Marine Geology*, 160, 147–170.
- Mari X., Torrétion J.-P., Trinh C.B.T., Bouvier T., Chu V.T., Ouillon S., Lefebvre J.-P. 2012. Seasonal aggregation dynamics along a salinity gradient in the Bach Dang estuary, North Vietnam. *Estuarine and Coastal Shelf Sciences*, 96, 151–158.
- Matsunaga N., Sugihara Y., Komatsu T., Masuda A. 1999. Quantitative properties of oscillating-grid turbulence in a homogeneous fluid. *Fluid Dynamics Research*, 25, 147–165.
- Markussen T.N., Andersen T.J. 2013. A simple method for calculating in situ floc settling velocities based on effective density functions. *Marine Geology*, 344, 10–18.
- Mietta F., Chassagne C., Winterwerp J.C. 2009. Shear-induced flocculation of a suspension of kaolinite as function of pH and salt concentration. *Journal of Colloid and Interface Science*, 336, 134–141.
- Neukermans G., Loisel H., Mériaux X., Astoreca R., McKee D. 2012. In situ variability of mass-specific beam attenuation and backscattering of marine particles with respect to particle size, density, and composition. *Limnology and Oceanography*, 57(1), 124–144.
- Passow U., Shipe R.F., Murray A., Pak D.K., Brzezinski M.A., Alldredge A.L. 2001. The origin of transparent exopolymer particles (TEP) and their role in the sedimentation of particulate matter. *Continental Shelf Research*, 21, 327–346.
- Raudkivi A.J. 1976. *Loose Boundary Hydraulics*, 2nd ed., Pergamon, New York.
- Rochelle-Newall E.J., Mari X., Pringault O. 2010. Sticking properties of transparent exopolymeric particles (TEP) during aging and biodegradation. *Journal of Plankton Research*, 32(10), 1433–1442.
- Traykovski P., Latter R., Irish J.D. 1999. A laboratory evaluation of the LISST instrument using natural sediments. *Marine Geology*, 159, 355–367.
- Tsujimoto T. 2010. Diffusion coefficient of suspended sediment and kinematic eddy viscosity of flow containing suspended load. *River Flow 2010 - Dittrich, Koll, Aberle & Geisenhainer (eds)*, 801–806.
- Van der Lee E.M., Bowers D.G., Kyte E. 2009. Remote sensing of temporal and spatial patterns of suspended particle size in the Irish Sea in relation to the Kolmogorov microscale. *Continental Shelf Research*, 29, 1213–1225.
- Van der Lee W.T.B. 2000. Temporal variation of floc size and settling velocity in the Dollard estuary. *Continental Shelf Research*, 20(12–13), 1495–1511.
- Verney R., Lafite R., Brun-Cottan J.-C. 2009. Flocculation potential of estuarine particles: the importance of environmental factors and of spatial and seasonal variability. *Estuaries and Coasts*, 32, 678–693.
- Voulgaris G., Meyers S.T. 2004. Temporal variability of hydrodynamics, sediment concentration and sediment settling velocity in tidal creek. *Continental Shelf Research*, 24, 1659–1683.
- Winterwerp J.C. 1998. A simple model for turbulence induced flocculation of cohesive sediment. *Journal of Hydraulic Research*, 36(3), 309–326.
- Winterwerp J.C. 2002. On the flocculation and settling velocity of estuarine mud. *Continental Shelf Research*, 22, 1339–1360.